Analysis of Emphysema Patterns in Computed Tomography Images

[1]Musibau Adekunle Ibrahim, [2]Oladotun Ayotunde Ojo, [2]Peter Adefioye. Oluwafisoye

[1]Department of Information and Communication Technology. Osun State University, Osogbo, Nigeria
[2.]Department of Physics,Osun State University, Osogbo, Nigeria

Abstract— Texture analysis and classification is one of the biggest challenges in the field of computer vision and pattern recognition. In this case, fractal dimension (FD) has proven to be a useful technique to characterize distinctive texture patterns. However, it could be sometimes difficult to use this approach to extract descriptors as the fractal magnitude space usually fails in representing adequately the richness of detail present in a unique feature vector. This paper proposes two new methods for emphysema patterns analysis and detections. The first approach is the Higuchi fractal dimension, different methods of calculating the Higuchi's dimension of digital images would be used in this paper for identifying the region of interest (ROI) in images. The second idea applied the multi-fractal spectrum for efficient identification of emphysema patterns in high resolution computed tomography (HRCT) images. The multi-fractal spectrum is a graphical representation of FD values in different regions within the images, which can be used as a global descriptor for accurate pattern recognition. The proposed algorithms have been applied to identify the locations and corresponding quantity of the emphysema patterns in HRCT images. Some of the experimental analyses of the results are investigated using the statistical analysis to establish the relationship between the ground truth patches and the HRCT image slices. It was concluded that the Higuchi's dimension and the multi-fractal analysis can be accurately used for detecting the regions with emphysema patterns.

Index Terms— Multi-fractal analysis, Holder exponent, fractal dimension, self-similarity properties, emphysema patterns.

———————————— u ————————————

1 INTRODUCTION

Fractal dimension plays a central role in the theory of fractals and also in almost all applications involving fractals. Fractal dimension has the ability to characterize the irregularity of shapes, which other dimensions such as the topological dimension may not be able to represent. The fractal dimension is used to estimate the size and roughness of fractal sets; it is a number associated with a fractal that tells how densely the fractal occupies the underlying space. The computational methods that can be used for the estimation of fractal dimension are the box counting and the Higuchi methods.

The fractal systems can fall into the category of mono-fractals whose characteristics are represented by a single exponent called the fractal dimension. This concept can be generalized into a wider and more complex multi-fractal system characterized by a continuous spectrum of exponents (called the singularity spectrum or multi-fractal spectrum). Thus, a multi-fractal system can be thought of as a combination of several fractal systems collectively exhibiting a variation of fractal dimensions at different scaling exponents. However, it should be noted here that multifractal analysis has not been used to characterize or identify multiple self-similar structures in an image. Since a fractal property can be considered as a statistical representation of roughness of the objects, a more general multifractal descriptor encodes the statistical distribution of irregularities in an image, which can be used as just texture feature descriptors for image analysis applications. Much work has been done on the region of interest identification by using the general or classical approaches [1],[2] but not in multi-fractals. Multi-fractal features have been successfully used as a global descriptor for efficient classification in biomedical images. A method for identifying the region of interest in a mammogram image was developed by [3], and in [4], a model for multi-fractal analysis has been proposed for automatic detection of microcalcification in tissue images.

This paper therefore proposes two methods for efficient recognition of the emphysema patterns; the implementation of the Higuchi's dimension and the multi-fractal analysis of the image intensity. The proposed system would focus on detecting the emphysema patterns by identifying the patterns within the images using some of the characteristic parameters in the extracted features. The proposed ideas can be achieved in various ways; the absolute differences in the overall mean values of the Higuchi's FD values between the normal tissue images and the histological images could be used. The regions with the statistically significant absolute mean differences contain the emphysema patterns while the regions without significant differences have no emphysema patterns. In the case of multi-fractal, the same procedure can be used to differentiate between the regions with emphysema patterns and those regions without patterns.

2 PREVIOUS WORK

The applications of fractal dimensions have also been previously used to locate and identify regions of interest in various digital images [5], [6],[7]. The complexities of the images within different locations can be varied with different measures of fractal dimensions; the regions or sections with the emphysema in the CT images, for instance, are expected to be more complex than the

other regions without, and would have higher values of fractal dimensions.
The author in [8] applied the multi-fractal characterizations of the images for edge detection. The process was achieved by using the smoothing process, which is tantamount to the inverse of a classical approach. The good thing about this process is that the information is neither lost nor introduced. The results of the segmentation are very excellent. One of the limitations in this case is that the computational complexity is very high. In this paper, the multi-fractal analysis was introduced to detect micro-calcifications. This was done by calculating the multi-fractal analysis and segmenting the images in an interactive manner in order to find suspicious regions. The problem with this approach is that the segmentation method that was introduced may not be able to detect patterns of diseases like emphysema since it is not visible like micro-calcification or other visible nodules.
Higuchi fractal dimension has also been used to diagnose patients with an Alzheimer disease. HRCT is a very effective scanning method that is more sensitive than chest radiography in measuring the type, extent and distribution of emphysema. Some patients with early emphysema, particularly those with early disease might still have the symptoms and this is the stage where HRCT is most useful.
Emphysema in HRCT is characterized by the presence of areas of abnormally low attenuation, which can be easily contrasted with surrounding normal lung parenchyma [9],[10],[11],[12]. Emphysema can be classified into three different classes: (i) centrilobular emphysema (CLE), defined as multiple small low-attenuation areas, (ii) paraseptal emphysema (PSE), defined as multiple low-attenuation areas in a single layer along the pleura often surrounded by interlobular septa that is visible as thin white walls, and (iii) Panlobular emphysema (PLE), defined as a low-attenuation lung with fewer and smaller pulmonary vessels [9].
Previous studies have shown several ways by which the CT imaging could be used for early detection of emphysema in patients with COPD [13]. HRCT of early centrilobular emphysema (CLE) shows uniformly distributed tiny areas of low attenuation while in panlobular emphysema; HRCT shows either panlobular low attenuation or ill-defined diffuse low attenuation of the lung. Paraseptal emphysema (PSE) is characterized by subpleural well-defined spaces [14].
The paper by Masashi [14] comprehensively described emphysema diseases, different classification of emphysema and their properties. It was also demonstrated that features from HRCT images could form important quantitative measures for identifying different classes of emphysema and the assessment of their severity.
The Holder exponent of the local distribution of the intensity measure has been previously implemented and applied for the development of multi-fractal spectrum in CT images [15],[16],[17], [18],[19],[20],[21].
The computation of a multi-fractal descriptor depends on the calculated Holder exponent and fractal dimension, which have been successfully used as a global descriptor for efficient classification in biomedical images. A method for identifying the ROI in a mammogram image was developed by [3] . In [2], a model for multifractal analysis has been proposed to assist the radiologist in diagnosing the breast cancer. In this case, the regions containing the cancer nodule were identified and the developed system presents very good classification accuracy in distinguishing the nodules locations between the regions with cancer and the regions without.
Dubey and Singh [22] introduced a novel feature descriptor called Local Bit-Plane Decoded Pattern and used it for biomedical image indexing and retrieval. Their experimental performance analysis using the 168 patches from the emphysema database showed an average retrieval precision (ARP) of approx. 75% and average retrieval rate (ARR) of 88%. A similar image retrieval system using local gray scale invariant features was proposed by [23] where they achieved an ARP of approx. 90% and an ARR of approx. 52%. However, in this study, they used only 37 HRCT slices containing the lower part of the lung.
The Higuchi's dimension for different channels of EEG signals was applied to identify the regions with Alzheimer's disease (AD) [24]. The results showed that the AD patients have significant lower Higuchi fractal dimension values when compared with the normal subjects. In [25], multifractal analysis has been successfully used to separate EMG signals with fatigue conditions from those without fatigue conditions. The multifractal analysis extracted the characteristics of EMG signals for this comparison and the results demonstrated that the strength of multifractality is very high as the differences between the EMG signals with fatigue conditions and nonfatigue regions are highly significant. Kara and Ertas [26] applied Uroflowmetry test to evaluate urine flow rates and volumetric analysis of patients. The Higuchi's fractal dimension computation for Uroflowmetry signals of both abnormal and normal patients was implemented for analysing and investigating the characteristics of these signals. Multifractal analysis has been applied for various applications in biomedical images and the results accomplished so far demonstrated the strength and capability of multifractal features [27]. In this paper, the introduction of Higuchi's dimension would help us to evaluate the performances of the local descriptor in the analysis of the emphysema patterns while the multi-fractal analysis could be used for global descriptions of the image features.

3 EXPERMENTAL DESIGN FOR EMPHYSEMA DETECTION

The Higuchi's method is an efficient way of calculating the fractal dimension of a curve that has found several applications in the analysis of time series. Higuchi's method is particularly suitable for a one-dimensional signal whose values at regular discrete intervals are available in the form $x(i),\ i = 1, 2, \ldots N$. Several new data point series are constructed using an interval length d, and starting value index m:

$$S_m(d) = \{ x(m),\ x(m+d),\ x(m+2d),\ \ldots x(m+pd) \} \quad (1)$$

Where

$$P = \left\lfloor \frac{N-m}{d} \right\rfloor \quad (2)$$

The length of the series in $Sm(d) = \{ x(m),\ x(m+d),\ x(m+2d),\ \ldots x(m+pd) \}$

(1) is calculated as a normalized sum of differences:

$$Lm(d) = \frac{N-1}{pd^2} \sum_{i=1}^{p} \left| x(m+id) - x(m+(i-1)d) \right| \quad (3)$$

The mean length for each interval length d is obtained as

$$L(d) = \frac{1}{d} \sum_{k=1}^{d} L_k(d) \quad (4)$$

As in the case of the box-counting dimension, the Higuchi dimension D_H is also computed as the slope of a linear regression line obtained using a log-log plot with *log(d)* along the *x*-axis, and *log(L(d))* along the *y*-axis.

An *NxN* image *I*(*i*, *j*) must be converted to one-dimensional data before the above method can be applied. A common approach used for this is to add the values along each column to get a one-dimensional array of sums of pixel intensities:

$$x(i) = \sum_{j=1}^{N} I(i,j), \qquad j=1,2,..N. \quad (5)$$

In Higuchi's dimension, the procedures for the extraction could be accomplished by using the horizontal row data of the image slice or the vertical column data within the image for the computation of the Higuchi fractal dimension. The corresponding values for each row or column would be used to determine the slice or region that contains the emphysema patterns.
In this section, the Higuchi's dimension has been implemented and applied for detecting the regions with or without emphysema patterns. The details of the procedures involving the detection of the emphysema regions using the Higuchi fractal dimension and the box counting are presented in Figure 1. The FD of subdivided images has been calculated by using the Higuchi method and the box counting method. The Higuchi of each sub-image is computed for the normal tissues and emphysema images. The magnitude of the differences in FDs between the normal and the emphysema classes (CLE and PSE) would determine the complexity of the images in those regions. The second part of the algorithm uses the box counting method for computing the FDs in different regions of the images in order to generate the multi-fractal spectrum. The deviation in the FDs between the NT and other classes in both approaches is the key to measure the tissue complexities that determine the quantity of the emphysema patterns in a particular region. The calculated Higuchi fractal dimension for each sub-image across the slice and the corresponding absolute differences are presented in the following section.

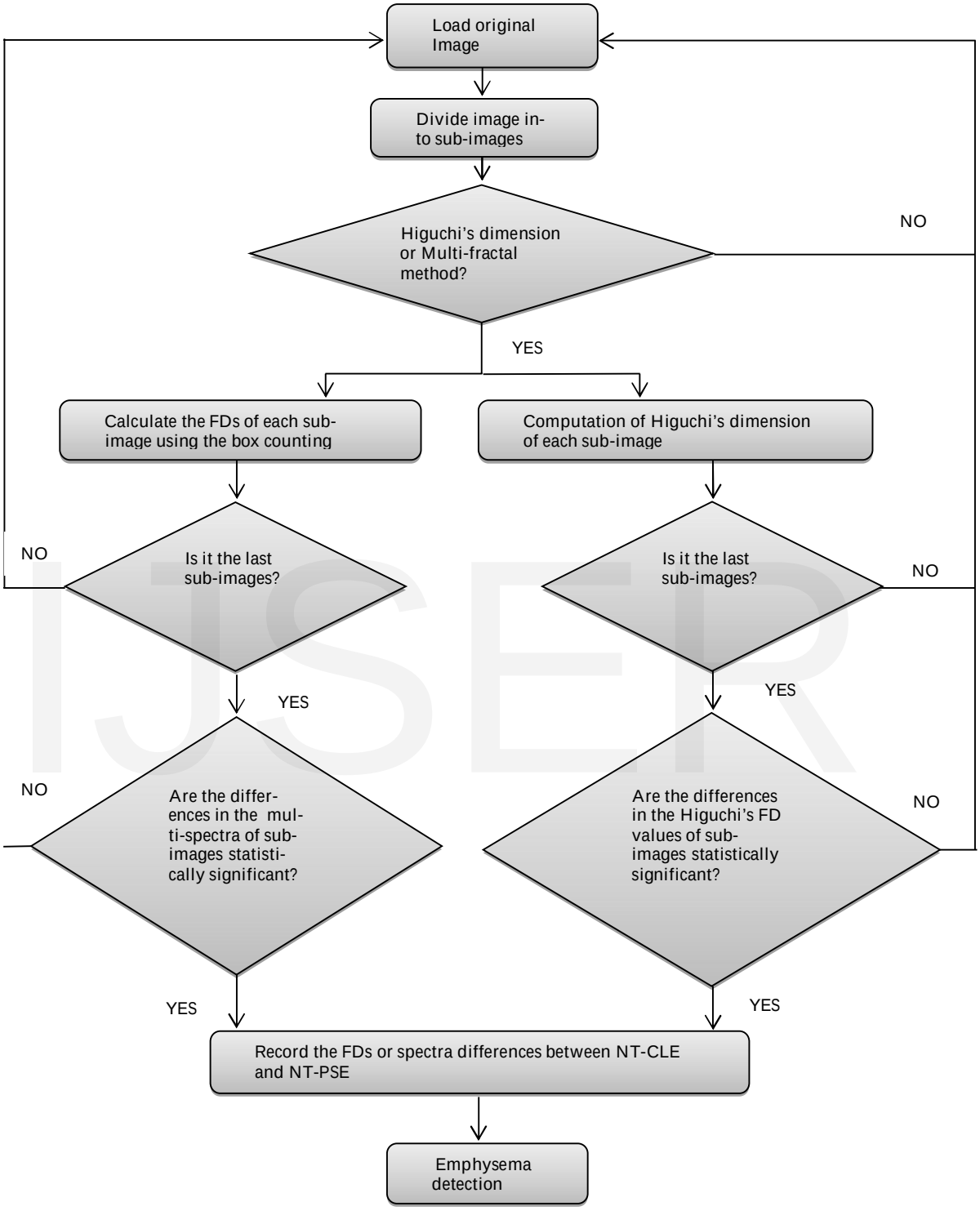

Fig. 1. System Overview of emphysema detection in HRCT images

4 Results and Discussion

The results of the experiments, which show the group means and the corresponding p-values for each experiment are shown in

Table 1. In each group, it has been established that the values of the group mean between the emphysema class of the ground truth images and the corresponding sub-images extracted from the slices overlap each other and even the corresponding p-values in each test show that there is no significant differences between the images.

TABLE 1
INTRA-CLASS VARIATION BETWEEN THE PATCHES AND CORRESPONDING SUB-IMAGE SLICES

Patches/Slices	Mean1	Mean2	P-values
NT1-NT1	1.9915	1.9949	0.2947
CLE1-CLE2	1.9915	1.9961	0.2907
PSE1-PSE1	1.9925	1.9965	0.2919

The visual representation of the multi-comparison results demonstrating the graph of the estimates with comparison intervals between the group means of the normal tissues of the ground truth images and the image slice sub-regions are presented in Figure 2.

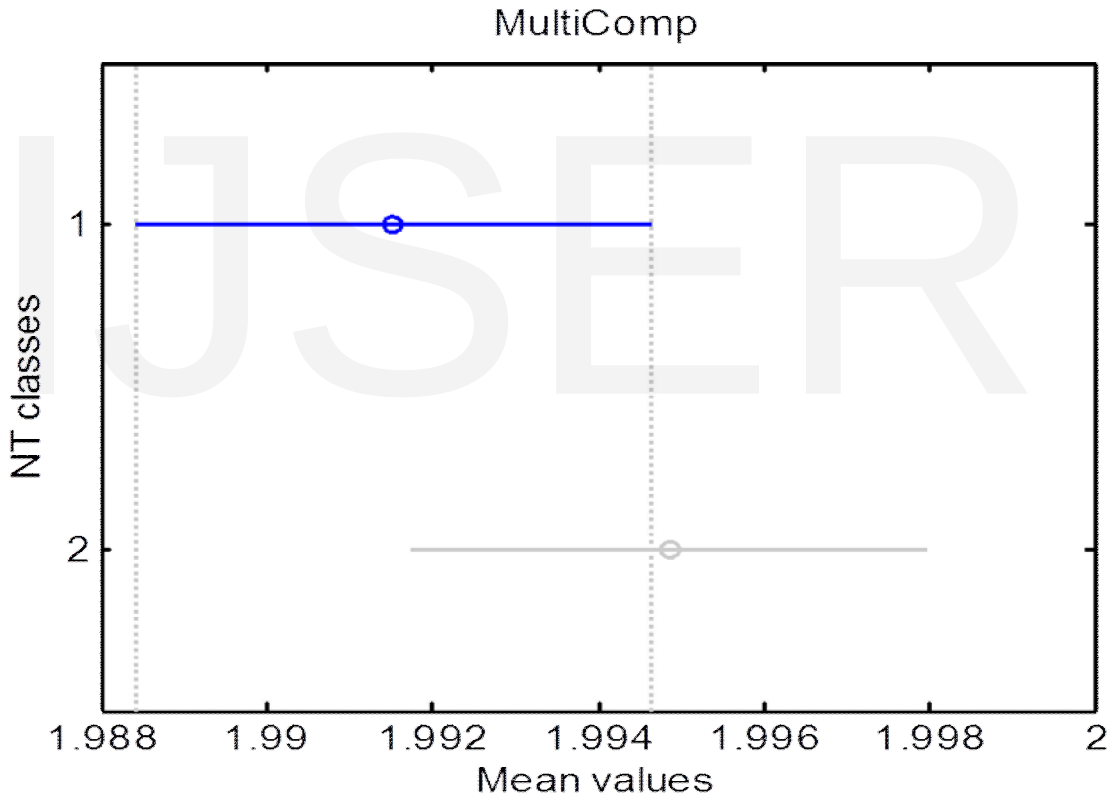

Fig. 2. Group means between the normal tissues of the ground truth and sub-regions of slices.

Each emphysema image is subdivided into 12 sub images and the differences in FD for each sub image is calculated between the normal image and the images with the emphysema patterns. The calculated Higuchi fractal dimension for each sub-image across the slice and the corresponding absolute differences are presented in Table 2. The results presented in Table 2 show that the FD differences between the normal and emphysema images (CLE and PSE) range between 0.0258-0.7082 and 0.0105-0.3525 for the NT-CLE and NT-PSE respectively. It is noted that the differences in FDs values are statistically significant at some regions but not statistically significant in some other regions.

The differences in the FDs in the regions that are statistically significant using the analysis of variance (ANOVA) indicate the presence of emphysema, with a p-value < 0.0001. The NT-CLE range of FD differences detects more presence of emphysema than the NT-PSE. Although, very large FD differences in both CLE and PSE show the presence of large emphysema in the images.

TABLE 2
HIGUCHI FDS OF EMPHYSEMA IMAGES

FD of the emphysema images using the Higuchi dimension method					
M. Locations	NT-FD	CLE-FD	PSE-FD	|(NT-CLE)|	|(NT-PSE)|
E11	1.114	1.0734	1.145	0.0406	0.031
E12	1.3131	1.5	1.0299	0.1869	0.2832
E13	1.2569	1.3059	1.0661	0.049	0.1908
E14	1.0982	1.0724	1.2018	0.0258	0.1036
E21	1.0982	1.8064	1.4507	0.7082	0.3525
E22	1.4198	1.507	1.3635	0.0872	0.0563
E23	1.5987	1.3909	1.5404	0.2078	0.0583
E24	1.5478	1.4341	1.4494	0.1137	0.0984
E31	1.1505	1.1799	1.161	0.0294	0.0105

This result also indicates that a large number of image subdivision is important for the detection and location of emphysema images, take for instance, it was verified experimentally when the whole HRCT image is divided into four sub images, the differences in the FD is not much between the Normal and the emphysema images, the differences in FD are not statistically significant, but an increase in the number of image subdivisions could improve the detection accuracy since the emphysema will usually occupy small position within the images. The reason for estimating the FD of different parts of the HRCT images is because higher FD values could be associated with tissue complexity due to the presence of emphysema. In all cases, the parts of the image with emphysema showed significantly higher FD values compared to the regions without FD values.

The overall result in Table 2 has been very good in terms of detecting the emphysema; the regions that clearly indicate the presence of emphysema are those where the Higuchi FD differences are statistically significant. The detections of the emphysema in the CLE image can be observed in different regions compared to the PSE image and they are of different quantities since the quantity of the emphysema detected directly depends on the magnitude of the FD differences between the normal and the emphysema images. The exact position of the emphysema can be identified by using the FD differences, but in the Table 2, the changes in FD between the normal and emphysema images in the cell locations (1,2 and 2,1) are statistically significant in PSE image and only cell location 1,2 in CLE image. These significant differences indicate the presence of emphysema patterns in these locations. The remaining locations fail to show the presence of emphysema since the changes in FD vary only in the range of 1-2% and the variations in FD are not statistically significant. Generally speaking, the FD values in the cell locations in the normal images are less than the CLE images and that of the CLE images are less than the PSE images.

Though, this is not true in some locations, but in most cases as presented in Table 2, the higher the complexities of the image tissues, the higher the FD values of the corresponding locations and thus the higher the presence of the emphysema in that location. The visualization of the FDs values for the three classes of the emphysema images are plotted against the corresponding sub images and the results are presented in Figure 3. This is in line with the previous explanations, the 12 sub-images number on the x-axis is when the image slice is arranged from left to right and from top to bottom. The FD values of the CLE sub-images are more discriminating in some sub-images, especially among sub-images 2, 5 and 11 than others, and the FD values of the normal NT slice are generally lower than the pathological images apart from the sub image 7 when its FD value is higher than the corresponding FD value of the PSE.

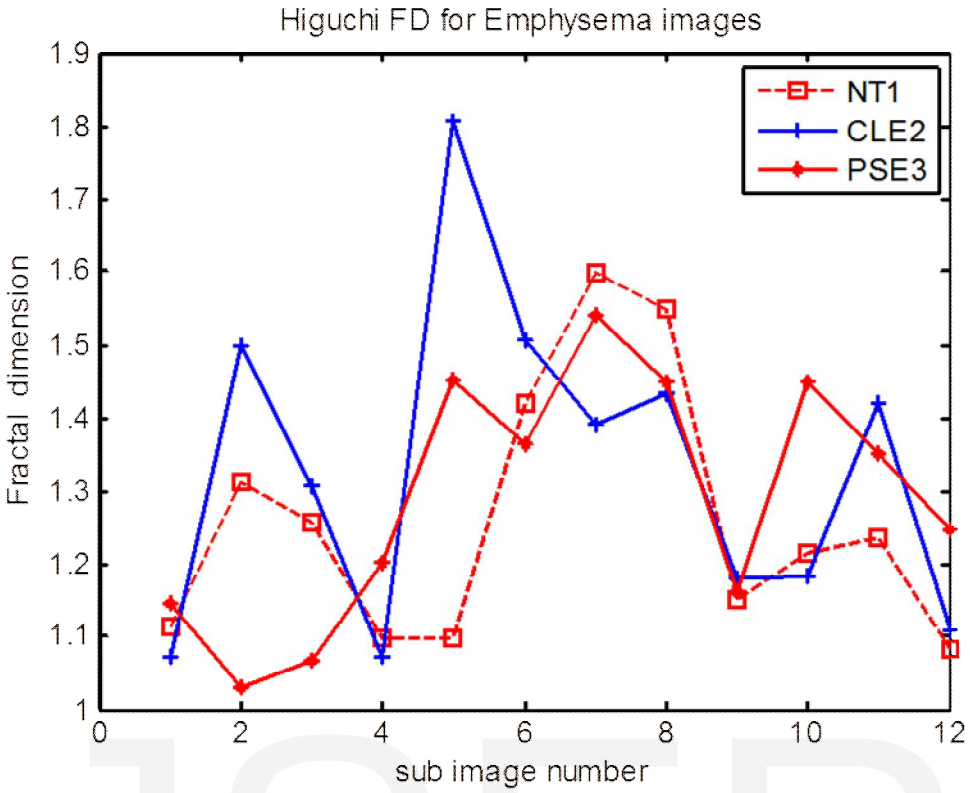

Fig. 3. FD of CT emphysema images against the corresponding sub-image number.

In Figure 4, the FD differences between the normal image and the emphysema images are plotted against sub-images. The normal NT-CLE has higher FD differences than the NT-PSE in some sub-images while the NT-PSE also has higher FD differences in few sub images than NT-CLE. This means there is a presence and detection of more emphysema patterns in the CLE than the PSE image slice since the FD differences in NT-CLE are generally higher in most sub-images than that of NT-PSE.

Another procedure that would be investigated is to compare the calculated multi-fractal spectra of each sub-image slice in order to determine the location and the presence of the emphysema by using the shape generated by the multi-fractal spectrum. Multi-fractal can be described as the generalization of fractal dimension, that is, it would calculate the FDs at the different step interval.

The multi-fractal method for detecting the ROI of the HRCT images has been implemented using the box counting method, the calculated FD of different regions of the image slice has been used for the computation of the multi-fractal spectrum.

The experiments were conducted using the multi-fractal methods on the same sub-divided images of the CLE used in the Higuchi method. It was discovered that the locations with the presence of emphysema in the Higuchi method, that is, the regions with the largest FD differences when compared with the normal images also gave the best spectra in the multi-fractal.

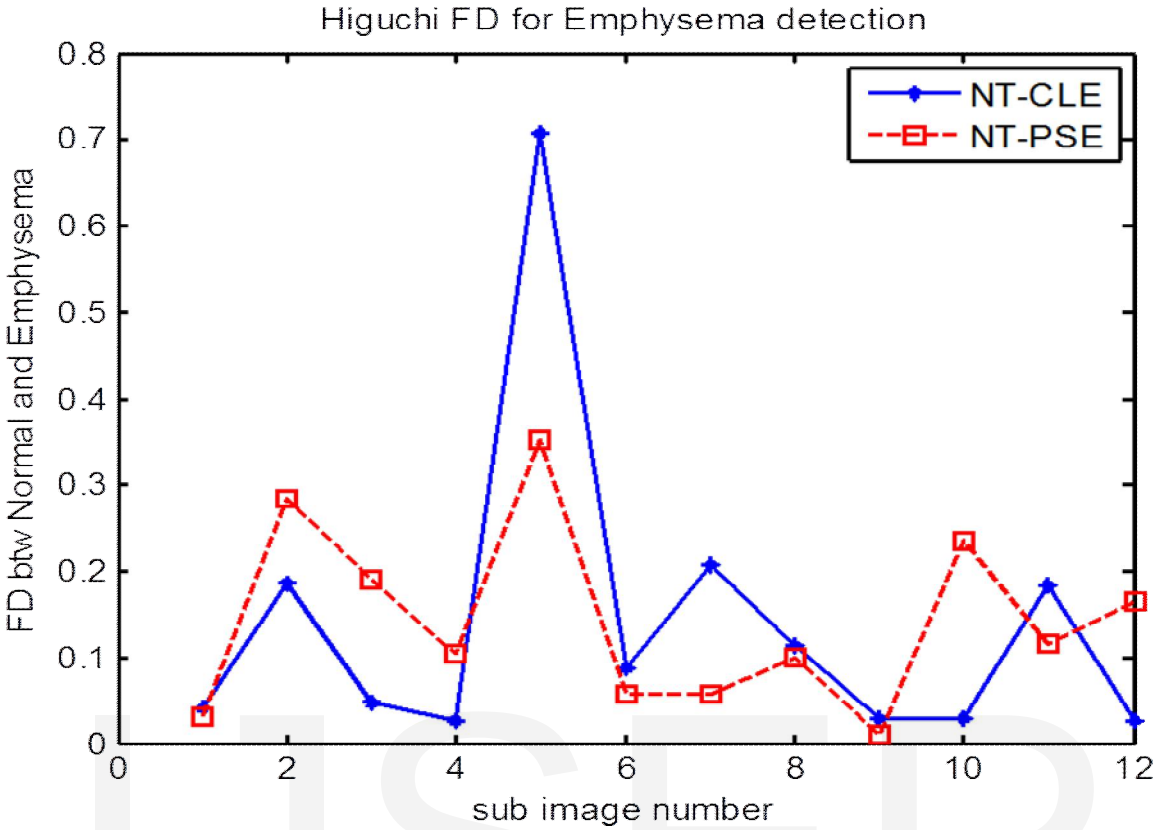

Fig. 4. FDs differences between the NT and the pathological images.

For instance, the results of the multi-fractal spectra for the sub-images at the matrix locations 1,2, 2,1 and 3,2 are shown in Figure 5b while other regions are considered as noise. For example, the multi-fractal spectra of other three selected regions without emphysema are presented in Figure 5a, as can be seen; the spectra in Figure 5a are not as clean as the spectra in Figure 5b. Furthermore, the higher the Higuchi FD values as shown in Table 2, the better the spectrum of the corresponding sub-images. For example, the multi-fractal spectrum of the image with the highest Higuchi FD (FD = 1.8064) is better than the spectra of the images with the FD values of 1.5 and 1.1834, and would automatically detect more emphysema than other spectra with lower FD values.

In Figure 5, the spectra in the first row for the sub images (Figure 5a) are smaller than the spectra of the sub-images with the presence of emphysema (Figure 5b). The Holder exponent alpha ranges from 1.5 to 2.1 ($\alpha_{max} - \alpha_{min}$) in the regions without emphysema while the alpha ranges from 1.4 to 2.7 ($\alpha_{max} - \alpha_{min}$) in the case of the regions with the detection of emphysema. It was observed that the sizes of the multi-spectra in the images with emphysema are generally larger than the sizes of the spectra with the images without emphysema; therefore, singular exponent alpha is an important parameter in the identification and detection of emphysema. This is in line with the results in Table 2 that uses Higuchi dimension for the computation of fractal dimension. The higher the FD values of the region the greater the multi-fractal spectra of the regions, the greater the detection and the identification of the emphysema.

On the other hands, the regions with higher FD values or greater spectra would detect more emphysema than the regions with lower FD values or smaller spectra. This is an indication that the fractal dimension in the case of emphysema CT regions has singularities degree higher than the normal case or the regions without emphysema.

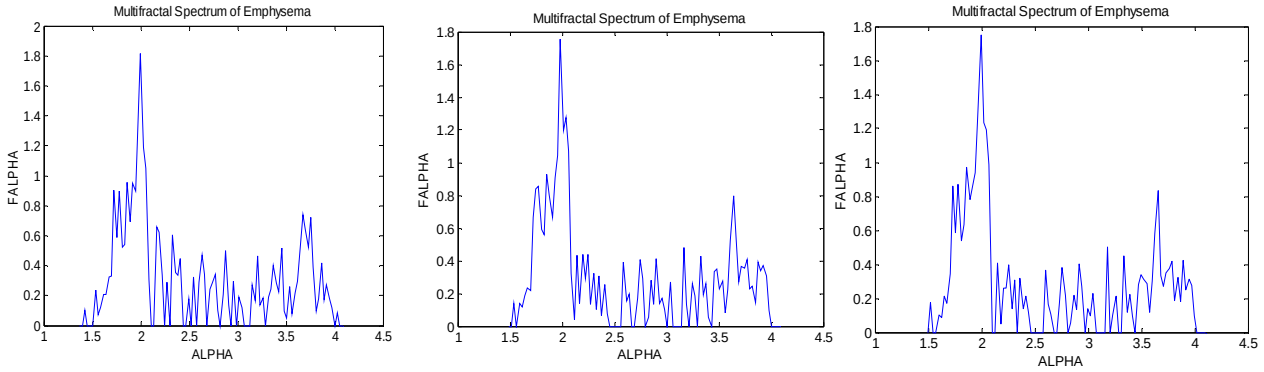

(a) Multi-fractal Spectra of the Normal regions

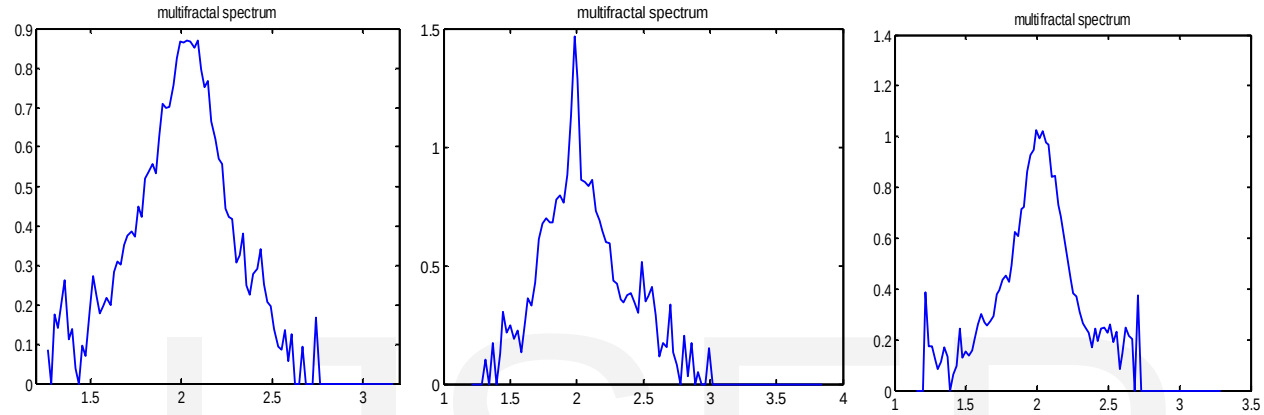

(b) Multi-fractal spectra of the emphysema regions.

Fig. 5. Multi-fractal spectra of PSE sub-images.

The higher FD values or multi-spectra with larger high and width in some sub-images are due to the complexities of the tissue in that region due to the presence of emphysema. The degree of the singularities exponent can also be used to determine how severe the presence of emphysema in the region is? It has been noted that the spectra of all sub-images without emphysema are exactly the same such that any deviation of a spectrum away from the normal spectrum would indicate the presence of emphysema in that region. The details of the process of detecting emphysema in CT images using the calculated multi-fractal spectra are presented in Figure 6. Distinct deviations can be observed between the spectra of the normal image and the pathological images in terms of the minimum and maximum values of local and global information (α, f(α)). This deviation is an indication of the presence of emphysema in that sub-image as can be seen in Figure 6.

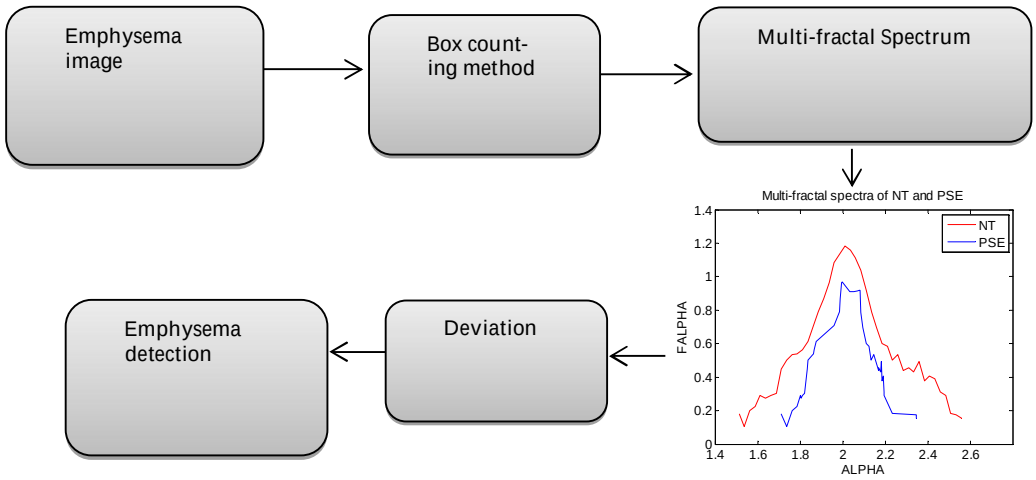

Fig. 6. System overview of the emphysema detection using the box counting method

5 Conclusions

The research work in this paper has presented some of the applications of fractal dimension in CT emphysema images. The Higuchi fractal dimension of the CT image has been used to identify and detect some of the regions of the image with the presence of emphysema.

It was discovered that the regions with the higher values of FD contain the presence of emphysema due to the image tissue complexities within the regions, while the detection of emphysema fails in those regions with lower FD values.

The multi-spectra obtained from the multi-fractal dimension computation showed the effectiveness of the global descriptions for identification and detection of ROI in HRCT images. The calculated spectrum parameters of HRCT images have been successfully applied to detect and identifying the regions with emphysema patterns in different types of lung tissue layers.

The useful features extracted from the image textures showed excellent performance. The methods demonstrated to be a very good measure and accurate enough to separate the regions with emphysema patterns from the regions without emphysema patterns. The results show that the multi-fractal spectrum of the CT images could also be used to detect the presence of emphysema as it is in line with the performance of the Higuchi's dimension.

Further research work could be done in this area by applying better methods in terms of accuracy and efficiency for calculating the fractal dimension of the CT images or improving the computational accuracy and time complexities of the algorithms. This research approach can also be further extended by applying Higuchi's method in a multi-fractal framework, such that the multi-fractal spectra of digital images can be calculated using the Higuchi's dimension and this can probably improve the recognition accuracy.

Acknowledgment

The authors would like to sincerely thank Associate Professor Mukundan, Department of Computer Science and Software Engineering at the University of Canterbury for his substantial contributions towards this study.

References

[1] S.A. Jayasuriya, A.W.C. Liew and N.F. Law, " Brain symmetry plane detection based on fractal analysis. Computerized Medical Imaging and Graphics, "37(7-8), pp. 568–580, 2013. doi:10.1016/j.compmedimag.2013.06.001

[2] F. Soares, F. Janela, M. Pereira, J. Seabra, and M. M Freire, "Classification of Breast Masses on Contrast-Enhanced Magnetic Resonance Images Through Log Detrended Fluctuation Cumulant-Based Multifractal Analysis," IEEE Systems Journal, 8(3), pp. 929–938, 2014.

[3] T. Stojić, I. Reljin, and B. Reljin, "Adaptation of multifractal analysis to segmentation of microcalcifications in digital mammograms.," Physica A: Statistical Mechanics and Its Applications, pp. 367, 494–508, 2006. doi:S0378437105012331

[4] Y. Ding, H. Dai, and H. Zhang, "Automatic detection of microcalcifications with multi-fractal spectrum", Bio-Medical Materials and Engineering, 24, pp. 3049–3054, 2014. doi:10.3233/BME-141126
[5] K. Iftekharuddin, K. M. Jia and R. Marsh, " Fractal analysis of tumor in brain MR images. Machine Vision and Applications, Springer-Verlag, " 13, pp. 352–362, 2003.
[6] Z.L. Jing, L.D. Zhang, and G.H. Yue, " Fractal dimension in human cerebellum measured by magnetic resonance imaging. Biophysical Journal," 85(6), pp. 4041–4046, 2003. doi:10.1016/S0006-3495(03)74817-6
[7] V. G. Kiselev, K.R. Hahn, and D.P Auer, "Is the brain cortex a fractal? NeuroImage, " 20(3), pp. 1765–1774, 2003. doi:10.1016/S1053-8119(03)00380-X
[8] J.L. Vehel, and P. Mignot, " Multifractal Segmentation of Images. Fractal World Scientific Publishing, " pp. 371–378, 1994.
[9] F. Chabat, G. Yang, and D. Hansell, "Obstructive lung diseases: texture classification for differentiation at CT Radiology,"228(3), pp. 871–877, 2003.
[10] C.S. Mendoza, G.R. Washko, J.C. Ross, A.A. Diaz, D.A. Lynch, and J.D. Crapo, " Emphysema Quantification in A Multi-Scanner HRCT Cohort using Local Intensity Distributions", IEEE, pp. 474–477. 2012.
[11] R. Nava, J. V. Marcos, B. Escalante-ram, G. Crist, and L.U. Perrinet, " Advances in Texture Analysis for Emphysema Classification. Springer-Verlag Berlin Heidelberg, " pp. 214–221, 2013.
[12] L. Sørensen, S.B. Shaker, and M.De. Bruijne, " Quantitative Analysis of Pulmonary Emphysema using Local Binary Patterns," IEEE Transactions on Medical Imaging, 29(2), pp. 559–569, 2010. doi:10.1109/TMI.2009.2038575
[13] E. Stern, S.J. Swensen, J.P. Kanne, "High Resolution CT of the Chest, Wolters Kluwer, " 2010.
[14] T. Masashi, J. Fukuoka, N. Nitta, R. Takazakura, Y. Nagatani, Y. Murakami, and K. Murata, " Imaging of pulmonary emphysema: a pictorial review. International Journal of Chronic Obstructive Pulmonary Disease," 3(2), pp. 193–204, 2008.
[15] A. Hemsley, and R. Mukundan, "Multifractal Measures for Tissue Image Classification and Retrieval. 11th IEEE International Symposium on Multimedia, " pp. 618–623, 2009. doi:10.1109/ISM.2009.94
[16] M. Ibrahim and R. Mukundan, " Multi-fractal Techniques for Emphysema Classification in Lung Tissue Images. International Proceedings of Chemical,Biological & Environmental Engineering," 78, pp. 115–119, 2014. Retrieved from http://www.etlibrary.org/?m=fbook&a=details&aid=15734
[17] M. Ibrahim and R. Mukundan, " Cascaded techniques for improving emphysema classification in computed tomography images. Artificial Intelligence Research," 4(2), pp. 112–118, 2015. doi:10.5430/air.v4n2p112
[18] R. Irini, B. Reljin, I. Pavlovic, and I.Rakocevic, " Multifractal analysis of gray-scale images. 2000 10th Mediterranean Electrotechnical Conference," Information Technology and Electrotechnology for the Mediterranean Countries. Proceedings. MeleCon 2000 (Cat. No.00CH37099), 2, pp. 490–493, 2000. Retrieved from www.worldscientific.com/doi/pdf/10.1142/S0218348X11005403
[19] M. Khider, B. Haddad , A.T. Ahmed, D. Technologie, H. Boumedienne, and B.P.B. Ezzouar, " Multifractal Analysis BY The Large Deviation Spectrum. International Workshop on Systems, " Signal Processing and Their Applications, 8, pp. 112–115, 2013.
[20] R. Mukundan, and A. Hemsley, "Tissue Image Classification Using Multi-Fractal Spectra. International Journal of Multimedia Data Engineering and Management," 1(2), pp. 62–75, 2010. doi:10.4018/978-1-4666-1791-9.ch006
[21] I.S. Reljin, and B.D. Reljin, "Fractal geometry and multifractals in analyzing and processing medical data and images", Archive of Oncology, 10(4), pp. 283–293, 2002. doi:10.2298/AOO0204283R
[22] S.R. Dubey, S.K. Singh, and R.K. Singh, "Local bit-plane decoded pattern: A novel feature descriptor for biomedical image retrieval," IEEE Jrnl. of Biomedical and Health Informatics, 20(4), pp. 1139-1147, 2016.
[23] M.A. Porto and M. d'Ornellas, "Automated Image Retrieval of Chest CT Images Based on Local Grey Scale Invariant Features. Studies in Helath Technology and Informatics," 2015.
[24] M. Prince et al., " Higuchi fractal dimension of the electroencephalogram as a biomarker for early detection of Alzheimer's disease ," 2015, World Alzheimer Report.
[25] K. Marri, R. Swaminathan , "Classification of muscle fatigue using surface electromyography signals and multifractals," Fuzzy Systems and Knowledge Discovery (FSKD) 12th International Conference on, pp. 669-674, 2015.
[26] S. Kara, M. Ertaş, C.P. Uzunoğlu, and A. Akan, " Fractal dimension analysis of Uroflowmetry signals, Signal Processing and Communications Applications Conference (SIU)," 25th, pp. 1-4, 2017.
[27] M. Ibrahim, "Multifractal Techniques for Analysis and Classification of Emphysema Images (PhD thesis)," University of Canterbury, 2017, http://hdl.handle.net/10092/14383.